Title
The Absence of Plasma in "Spark Plasma Sintering"

Authors
Hulbert, Dustin M.
Anders, Andre
Dudina, Dina V.
et al.

Publication Date
2008-11-15

The Absence of Plasma in "Spark Plasma Sintering"

Dustin M. Hulbert[1], André Anders[2], Dina V. Dudina[1], Joakim Andersson[2], Dongtao Jiang[1], Cosan Unuvar[1], Umberto Anselmi-Tamburini[1], Enrique J. Lavernia[1] and Amiya K. Mukherjee[1a)]

1. University of California, Davis, Department of Chemical Engineering and Materials Science, One Shields Avenue, Davis, CA 95616

2. Lawrence Berkeley National Lab, Plasma Applications Group, One Cyclotron Road, Berkeley, CA 94720

Spark plasma sintering (SPS) is a remarkable method for synthesizing and consolidating a large variety of both novel and traditional materials. The process typically uses moderate uni-axial pressures (< 100 MPa) in conjunction with a pulsing on-off DC current during operation. There are a number of mechanisms proposed to account for the enhanced sintering abilities of the SPS process. Of these mechanisms, the one most commonly put forth and the one that draws the most controversy involves the presence of momentary plasma generated between particles. This study employees three separate experimental methods in an attempt to determine the presence or absence of plasma during SPS. The methods employed include: in-situ atomic emission spectroscopy, direct visual observation and ultra-fast in-situ voltage measurements. It was found

using these experimental techniques that no plasma is present during the SPS process. This result was confirmed using several different powders across a wide spectrum of SPS conditions.

[a)] Electronic mail: akmukherjee@ucdavis.edu

I. INTRODUCTION

Spark plasma sintering (SPS) has emerged as one of the most effective sintering techniques in over a generation. SPS is quite similar to hot pressing (HP) in that a uniaxial pressure is applied across the specimen during the sintering process. However, the SPS process has a number of advantages over similar sintering methods such as HP. For one, materials can be sintered using SPS in a matter of minutes as opposed to hours or even days. Also, the requisite temperatures needed to consolidate to full density are significantly lower. This opens up the possibility to create materials with nanoscale structural features. Lastly, SPS is capable of sintering difficult-to-sinter materials such as tungsten carbide and hafnium diboride with relative ease and without the benefit of sintering aids.

SPS uses moderate uni-axial pressures (typically less than 100MPa) and an on-off DC pulsing current to sinter powders. Figure 1 shows a basic diagram of the SPS apparatus. During this on-off DC pulsing, there are a number of proposed mechanisms to account for the enhanced sintering behavior. Many of these mechanisms assume the presence of momentarily generated spark plasma between particles. Some of the proposed SPS mechanisms found in the literature are listed below.

1. Spark impact pressure .[1-3]
2. Plasma cleaning of particle surfaces [4, 5]
3. Joule (Rapid) heating [3, 4]

4. Local Melting and Evaporation (especially in metallic systems) [1]
5. Surface activation on the particles
6. Electron wind force [6]
7. Field assisted diffusion [2, 3, 5].

Of the mechanisms listed above, Joule heating and local melting and evaporation (in metallic systems) have been relatively well established. The other mechanisms, especially those that invoke the presence of plasma, are highly hypothetical in nature [7]. Other than sintering, SPS technology has been used to join materials, grow crystals, facilitate advanced chemical reactions and even form materials into different shapes [1, 8, 9]. A photograph of the SPS equipment sintering a nanocomposite ceramic oxide is shown in Fig. 2. For more information regarding the SPS process, Omori, Munir and Anselmi-Tamburini provide excellent reviews [1, 9]

However, despite over forty years of research and development there exists a large gap in the fundamental understanding of the spark plasma sintering (SPS) process and technological advances garnered by the process [9]. Without a fundamental understanding of the principle mechanisms at work during SPS it is expected that further advancements in the state of the art will be significantly delayed. This large gap in a fundamental understanding of process mechanisms has been filled with a variety of theories, many of which have yet to be experimentally verified [2].

Out of all of these theories, the ones that invoke the presence of plasma or a spark discharge are the most controversial. By utilizing in-situ atomic emission spectroscopy techniques, direct visual observation and ultra-fast in-situ voltage measurements in conjunction with choice starting powders this study attempts to shed some light on the plasma question.

The generation of metal or gaseous plasma occurs through ionization of metal atoms (e.g. Al, W, Cu) or gaseous molecules and atoms (e.g. O_2, N_2, H_2O, O, N, Ar, He). The ionization processes require the removal of at least one bound electron, which is generally done through electron impact ionization or Penning ionization [8, 10]. In both cases, the electron energy distribution function needs to have sufficient population of electron with energies exceeding the first ionization energy (which is typically on the order of 10 eV).

Ionization in metal and gas discharges is accomplished by (i) generating free electrons and (ii) accelerating them in electric fields to the energy necessary for ionization. The generation of free electrons can be related to thermionic emission, field emission, or a combination of both [11]. Whatever the case, locally strong fields must exist to facilitate electron acceleration and/or heating of the whole distribution.

In the plasma community, one distinguishes various forms and classes of discharges based on the macroscopic appearance, electrical parameters such as discharge voltage, discharge current, electron emission mechanism, and the frequencies of voltage and current changes. For example, three popular classes are arcs, sparks, and glow discharges [11]. Without going into an exhaustive discussion of these discharge classes, the authors only briefly state that sparks are characterized by a transient high current (often kA) and high voltage (often kV) [11]. Arcs have high current (typically 10 A or greater) and low voltage (typically 20 V) [11]. Glow discharges generally have low current (1 A or less) and relatively high voltage (300 V or more) [11].

Based on this rather superficial classification, we may already cast doubt that the plasma, should it exist in SPS, is of the spark type since that would require the presence of transient high voltages. The SPS works with power supplies of 5 V or less. This low applied voltage is in fact less than the required burning voltage for any of the above forms of discharges and therefore one would need to look for higher voltages that could be associated with the inductive generation given the high currents of the SPS process.

II. EXPERIMENTAL PROCEDURES

The experimental set-up for the in-situ atomic emission spectroscopy (AES) experiments is shown in Fig. 3. The equipment consists of a high temperature fiber optic flame probe (FL-400, Ocean Optics, USA) connected to a 2 m fiber

optic patch cable (Ocean Optics, USA) that is connected to a fiber optic ISO KF-40 vacuum feed-through (VFT-400-UV-40, Ocean Optics, USA). The fiber optic flame probe was sleeved in a borosilicate glass capillary tube to prevent damage to the probe during sintering. The glass sleeve lined a through hole located at the mid-plane of the die and was butted up against the powder charge.

In the case of metallic powdered specimens, the probe, along with the glass sleeve, were actually pressed into the powder charge with the tip of the probe located at the center of the specimen. Another 2 m fiber optic patch cable is then connected to a spectrometer (HR4000, Ocean Optics, USA), which is then connected to a PC for spectrometer data acquisition (Spectra Suite, Ocean Optics, USA). The spectrometer has a high photonic sensitivity of 130 photons/count at 400 nm and 60 photons/count at 600 nm with a RMS dark noise of 50 counts. In order to reduce the effects of dark noise the spectrographic integration time was set to 3.8 ms. Temperature was monitored using a K-type thermocouple seated in a near through-hole located at the center of the die. Prior to any SPS experiments involving a powder charge, a SPS spectroscopy experiment was carried out without a powder charge as a type of control experiment. This was done by placing a graphite ring spacer between the plungers and inserting the fiber optic probe through a hole drilled in the graphite ring. This placed the tip of the probe in the center of an empty cavity at the geometric center of the punch and die set-up.

In order to try and force a sparking event, a special experiment was designed using a standard SPS die and punch. Two copper plates where polished to a 45 μm diamond finished and a copper half cylinder was sandwiched between the two copper plates and the two punches. A schematic the experiment is shown in Fig. 4.

As is seen in Fig. 4 the fiber optic probe is placed directly adjacent to the point contact between the copper plate and the ground copper cylinder. Additionally, the sides of the punches in Fig. 4 were coated with boron nitride forcing all the current through the copper plates. The idea was to realize the highest current densities in a small region and therefore the greatest chance to detect plasma in this area.

In order to confirm the validity and accuracy of the fiber optic set-up the spectrometer was calibrated using the Na and K emission lines obtained exposing small amounts of KBr and NaCl salts to a gas flame.

Another experiment carried out involved using direct visual observation to try and detect any sparking or other anomalous visual radiation. This was done by loading the powders (or Cu plates and ground half - cylinder) into the die as before with in-situ AES experiments. However, instead of a through hole for the fiber optic cable, a 5.75 mm hole was drilled through the mid-plane of the die and a borosilicate glass mini test tube with an outside diameter of 5.73 mm was set in

the hole using zirconia paste. The base of the test tube was butted up into the powder charge. This effectively created a window through which the powder charge could be seen by focusing a telescope on the window. Fig. 5 illustrates the experimental configuration.

The voltage measurements between the upper and lower punches were made using a digital storage oscilloscope (Tektronix TDS 5104B, USA) with analog bandwidth of 1 GHz and sampling rate of 5×10^9 samples/sec. Each data capture was done with 4 million points spread over the duration of the processing burst. Al, Cu and Al_2O_3 powders were studied for this section of work. The wires were embedded in the powder charges and were approximately 1 mm – 3 mm apart. Voltage measurements were taken at two separate times during the SPS process. Sets of data were collected immediately after the current reached steady state (a few seconds after the on switch is pressed) and once the sintering temperature was reached.

This oscilloscope is one of the more sophisticated available and is capable of detecting events down to 200 ps. Such time resolution is desirable if one is trying to detect highly transient voltage anomalies associated with plasma, sparking or arcing events.

In order to avoid shorting the wires against the graphite dies and punches, alumina tubes were used as dielectric sheaths. A schematic of the set-up is shown in Fig. 6.

A wide variety powders and SPS conditions were this investigation. The list of powders used is large but included nanoscale powders and coarse powders with a variety of purities. These conditions and materials are summarized in Table I. Generally speaking, pressure was kept as low as possible as it was thought that this would maximize the presence of the point contacts and reduce plastic flow, which might decrease the likelihood of sparking events by increasing contact area (and hence reduce current density). The SPS apparatus used in this study was a Dr. Sinter 2050 (Sumitomo Coal Mining Co., Japan). Data such as temperature, pressure and displacement were monitored using a computer with a LabView (National Instruments, USA) program. All runs were executed using one heating step from room temperature to the desired sintering temperature. After the desired holding time had elapsed the power was shut off and the assembly was allowed to cool to room temperature. As mentioned previously, in some cases the current was forced through the powder charge by lining the sides of the die and punches with hexagonal boron nitride (Fig. 4). Also, in some experiments Ar at 96.3×10^3 Pa was used. However, for the majority of experiments, the atmosphere was a vacuum on the order of 5 Pa.

III. RESULTS

During all of the spectroscopy SPS experiments no characteristic photons were detected. Not even during the experiment involving the copper plates and the partially ground copper cylinder was any presence of plasma detected (see Fig. 5 and Table I). An example of what was detected is shown in Fig. 8.

The spectrum shown in Fig. 8 is for NaCl sintered at 650 ºC for 3 minutes. Fig. 8 is representative for all the SPS spectra taken during this investigation (including the control experiment with no powder charge). The details of this experiment and the other SPS runs are in Table I.

No spark, glow discharge or any other anomalous features were observed throughout the entire sintering process of all powders tested and during the Cu plate and Cu half-cylinder experiment.

Figs. 9 – 11 are for 325 mesh 99.9% pure Al powder after a temperature of 100 ºC was reached using a heating rate of 100 ºC/min. Similar plots were obtained for a Cu and Al_2O_3 powders across a variety of SPS process times and temperatures. No voltage anomalies associated with sparking, arcing or plasma generation were ever observed.

Since voltage measurements can be made with very high time resolution, data analysis by fast Fourier transform (FFT) is easily accomplished with digital data acquisition and processing. Acquired spectral power *P* can be evaluated using

the well-known theory of colored noise based on the fitting by a power law (Eq. 1) [12, 13]:

$$P(f) \sim 1/f^{\alpha} \quad (1)$$

Where f is the frequency and α is an exponent determining the color of the noise. The noise is white for $\alpha = 0$, i.e. independent of frequency, and pink for $\alpha = 1$. This is typical for systems of self-organized criticality [14]. The presence of plasma in the powder charges was investigated by recording the voltage with high band width and analyzing the time-dependent data by FFT (Fig. 9).

The period of the FFT shown in Fig. 9 includes one full duty cycle, which is approximately 35 ms on and 5 ms off. One clearly sees the fundamental frequency due to the rectifier properties of the power supply. The harmonics of power supply are also apparent. The dampened slope is due to the typical low band-pass filter properties of the measuring circuit. This filtering property is caused by the unavoidable inductance of the wires used during the experiment.

Figs. 10 and 11 show the voltage behavior of one process burst. Fig. 10 shows the potential across the powder charge and Fig. 11 shows the potential to ground voltage behavior.

IV. DISCUSSION

Suffice it to say, the AES results obtained do not speak favorably for the presence of plasma in the SPS. However, it is not possible to complete dismiss the possibility of plasma based solely on the AES results. If plasma is present during then it does not emit intense levels of radiation in the visible spectrum. Specifically, since the dark noise of the spectrometer is known, along with the photonic resolution, a calculation of how many photons a spark would have to generate in order to be detectable can be made. At 400 nm it would take approximately 104,000 quanta of photons to generate a detectable signal. This number decreases at 600 nm to approximately 48,000 photons. At 600 nm over 3.8 ms (the minimum integration time of the spectrometer) this corresponds to a power value on the order of 5×10^{-12} W.

Arguably, the most damaging piece of evidence for the case of plasma comes from the ultra-fast in-situ voltage measurements. While it can be argued that the experiments done using AES and the human eye are not sensitive enough, especially from a temporal stand point, the same cannot be said for the voltage measurements. With the exception of some special LASER induced plasmas, even the most transient of plasmas last for a few nanoseconds. With a temporal resolution of about 1 ns, the technique employed in this study would have detected any voltage transients necessarily associated with plasma events.

Regarding Fig. 9, the FFT plot shows that there are no high frequency components that could generate any discharge due to the possible inductive

components of the power supply or for that matter any possible radio frequency properties of the power supply. At approximately 5 kHz the harmonics of the power supply are fully dampened by the inductive nature of the sintering power circuit. The few “blips” that are visible at the higher frequencies (>100 kHz) are due to white noise. In other words, at the higher frequencies the signal's power spectral density has equal power in any band. While these signals may appear to be intense on the plot it is important to keep in mind the log – log nature of Fig. 9.

Fig. 10 shows that the voltage across the powder charge during the SPS process is less than 3 V. The 3 V measured by the oscilloscope is actually in good agreement with the non-time resolved voltage measurements of the SPS equipment itself. Fig. 11 is the time resolved potential to ground voltage of the SPS process. In this case the voltage is less than 1.5 V, which is logical given the less than 3 V across the punches (or electrodes). In both cases, the voltage is approximately one order of magnitude less than the required burning voltage of any form of electrical discharge for any material. There is simply not enough voltage (transient or otherwise) present in the SPS process to generate plasma.

The purpose of this investigation was to determine unambiguously the presence or absence of plasma during standard SPS operations using a variety of powders and sintering conditions. To that end, the authors have shown using three types of detection experiments that no plasma could be detected. Naturally, disproving

a hypothesis is in many ways more difficult than proving a hypothesis. However, if the plasma hypothesis is to gain serious traction, unambiguous evidence of its existence must be put forth in the open literature.

Regardless of the presence of plasma, SPS is a very attractive process and the effectiveness of the process remains unchallenged. For years, the hypothesis generally advanced for the superior sintering ability of the process has centered on the generation of momentary plasma between particles. The idea that plasma is in fact responsible for the SPS's remarkable abilities is now put in serious doubt. To that end, a portion of the "black box" label that has haunted the SPS process for so long can be partially removed.

Like most scientific inquires answering one question naturally leads to another question. In this case the most obvious question is: Given a lack of plasma, what is responsible for the enhanced sintering capabilities of the SPS? While the answer to this question goes beyond the scope of the present investigation some discussion is merited.

The fundamental underpinnings of the SPS method involve a rapid heating rate accompanied by pressure and high currents. Perhaps more attention should be given to these known salient features of the process. For example, enhanced sintering in conducting powder charges could be due in part to electromigration of point defects or other current effects [15]. Additionally, heating rate is known

to be a factor in determining the effectiveness of more traditional sintering methods [9, 16]. Also, Joule heating should be studied more in the context of SPS as its mechanistic existence is in little doubt. Clearly, more fundamental work is needed if the basal mechanisms responsible for the SPS's remarkable sintering abilities are to be had.

V. CONCLUSIONS

The existence of plasma was investigated using three methods:

1. In-Situ Atomic Emission Spectroscopy
2. Direct Visual Observation
3. Ultra-Fast In-Situ Voltage Measurements

Using a variety of powders and SPS conditions, all of the experimental methods employed indicate there is no plasma, sparking or arcing present during the SPS process, neither during the initial nor the final stages of sintering. The effectiveness of the SPS process to rapidly and efficiently consolidate a wide variety of materials with novel microstructures remains unchallenged. Other factors salient to the SPS process such as high heating rates may play a more important role than previously thought. More fundamental work into

understanding the underpinnings of the sintering mechanisms of the SPS process is still needed.

ACKNOWLDEGMENTS

This work is supported by the Office of Naval Research under Dr. Larry Kabacoff (Grants N00014-03-1-0148 and N00014-07-1-0745) and the Army Research Office under Dr. Sheldon Cytron (Grant W911NF-04-1-0348). Work by Berkeley Lab employees was supported by the U.S. Department of Energy under Contract No. DE-AC02-05CH11231.

References

1. Omori, M., *Sintering, consolidation, reaction and crystal growth by the spark plasma system (SPS).* Materials Science and Engineering A, 2000. **287**(2): p. 183-188.
2. Tokita, M., Journal of the Society of Powder Technology, 1993. **30**: p. 790-804.
3. Zhan, G.-D., et al., *A Novel Processing Route to Develop a Dense Nanocrystalline Alumina Matrix (<100 nm) Nanocomposite Material.* Journal of the American Ceramic Society, 2003. **86**(1): p. 200-2002.
4. Anselmi-Tamburini, U., et al., *Fundamental investigations on the spark plasma sintering/synthesis process: II. Modeling of current and temperature distributions.* Materials Science and Engineering A, 2005. **394**(1-2): p. 139-148.
5. Chen, W., et al., *Fundamental investigations on the spark plasma sintering/synthesis process: I. Effect of dc pulsing on reactivity.* Materials Science and Engineering A, 2005. **394**(1-2): p. 132-138.
6. Shewmon, P., *Diffusion in Solids*. 2 ed. 1989, Warrendale, PA: Minerals, Metals & Materials Society. 246.
7. Aldica, G., et al., *Electrical conduction in initial field assisted sintering stages.* Journal of Optoelectronics and Advanced Materials, 2007. **9**(12): p. 3863-3870.
8. Lieberman, M.A. and A.J. Lichtenberg, *Principles of Plasma Discharges and Materials Processing*. 1994, New York, NY: John Wiley & Sons.
9. Munir, Z.A., U. Anselmi-Tamburini, and M. Ohyanagi, *The effect of electric field and pressure on the synthesis and consolidation of materials: A review of the*

spark plasma sintering method. Journal of Materials Science, 2006. **41**(3): p. 763-777.

10. Smirnov, B.M., *Plasma Processes and Plasma Kinetics*. 2007, Weinheim, Germany: Wiley-VCH.
11. Anders, A., *Cathodic Arcs: From Fractal Spots to Energetic Condensation*. 2008, New York, NY: Springer, Inc.
12. Rosen, J. and A. Anders, Journal of Physics D: Applied Physics, 2005. **38**: p. 4184-4190.
13. Schroeder, M., *Fractals, Chaos, Power Laws: Minutes from an Infinite Paradise*. 8 ed. 2000, New York, NY: W.H. Freeman and Company.
14. Bak, P., C. Tang, and K. Wiesenfeld, Physics Review Letters, 1987. **59**: p. 381-384.
15. Bertolino, N., et al., *Electromigration effects in Al-Au multilayers.* Scripta Materialia, 2001. **44**(5): p. 737-742.
16. Olevsky, E., A. , S. Kandukuri, and L. Froyen, *Consolidation enhancement in spark-plasma sintering: Impact of high heating rates.* Journal of Applied Physics, 2007. **102**(11): p. 114913.

FIGURE CAPTIONS

Fig. 1 – A schematic of the SPS process.

Fig. 2 – The SPS in action consolidating an oxide ceramic nanocomposite.

Fig. 3 – The experimental set-up used during the in-situ AES investigations.

Fig. 4 – The configuration of the Cu plate – Cu half cylinder experiments. In this case, boron nitride was coated on the sides of the punches, forcing the current through the contact asperity were the fiber optic probe was located.

Fig. 5 – The experimental configurations used for the direct visual observations.

Fig. 6 – A diagram of the set-up used for the ultra-fast in-situ voltage measurements.

Fig. 7 – The results of the flame spectroscopy experiment used to calibrate the sensitivity and resolution of the equipment used in the in-situ AES experiments.

Fig. 8 – AES data for NaCl sintered via SPS. This plot is representative for all AES data collected during this study.

Fig. 9 – A FFT plot of one duty cycle of the SPS process. This plot is for the SPS of 325 mesh 99.9% pure Al powder after a temperature of 100 ºC was reached using a heating rate of 100 ºC/min. This plot is representative of all FFT data collected.

Fig. 10 – The voltage behavior of one process burst across the powder charge. This plot is for the SPS of 325 mesh 99.9% pure Al powder after a temperature of 100 ºC was reached using a heating rate of 100 ºC/min. This plot is representative of all FFT data collected.

Fig. 11 – The voltage behavior of one process burst from potential to ground. This plot is for the SPS of 325 mesh 99.9% pure Al powder after a temperature of 100 ºC was reached using a heating rate of 100 ºC/min. This plot is representative of all FFT data collected.

FIGURES

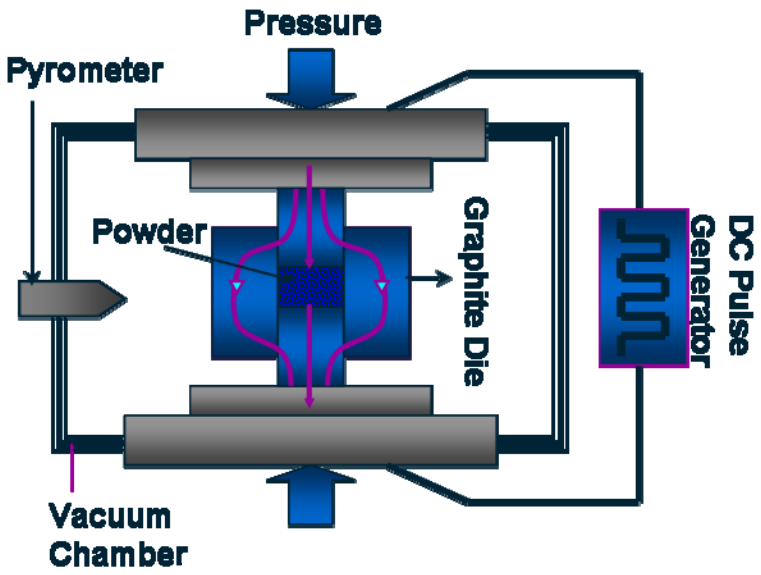

Fig. 1

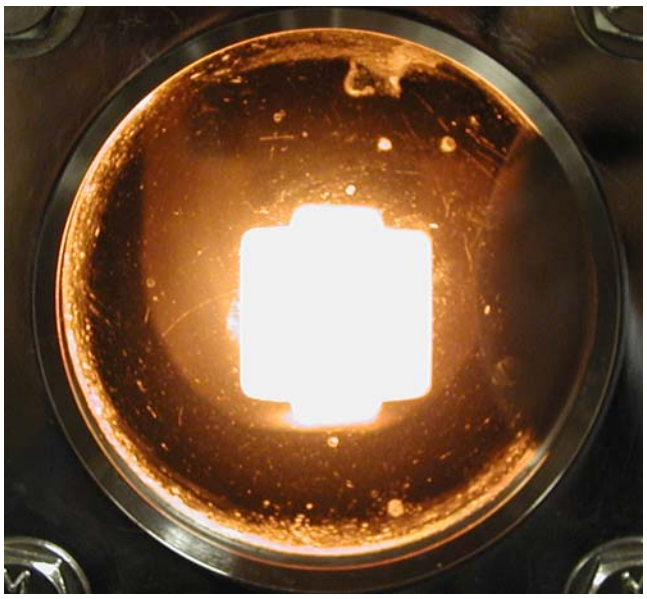

Fig. 2

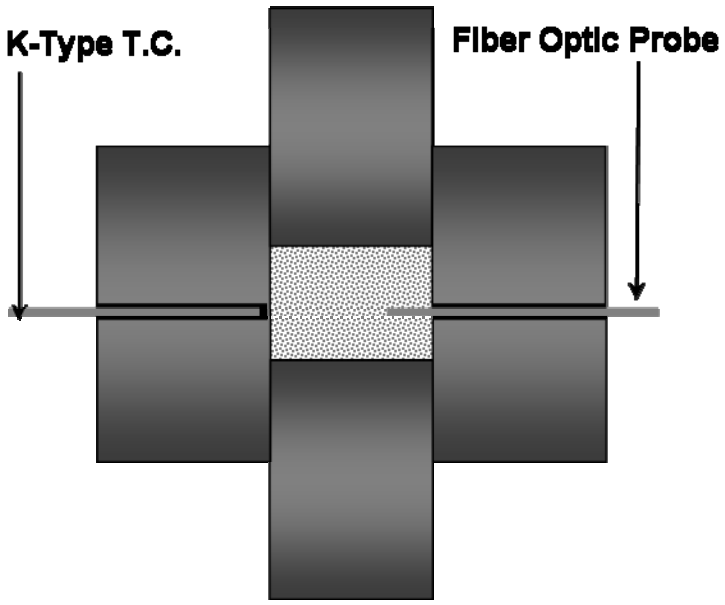
K-Type T.C.
Fiber Optic Probe

Fig. 3

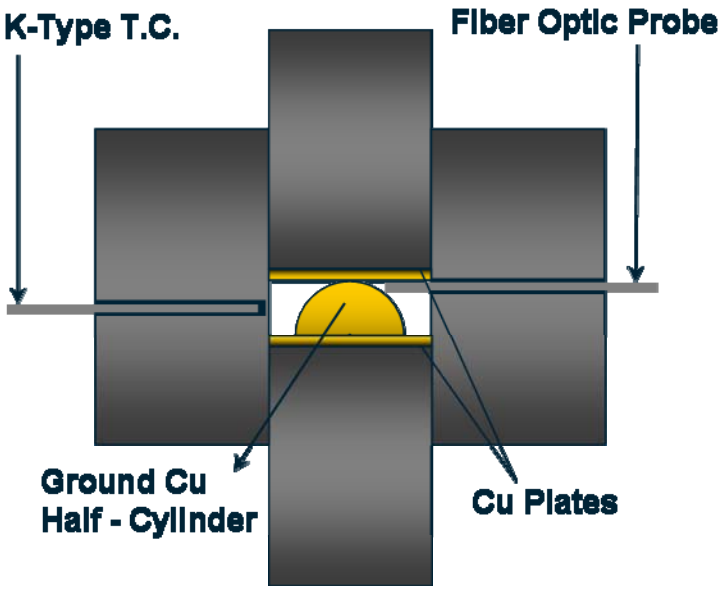
K-Type T.C.
Fiber Optic Probe
Ground Cu
Half - Cylinder
Cu Plates

Fig. 4

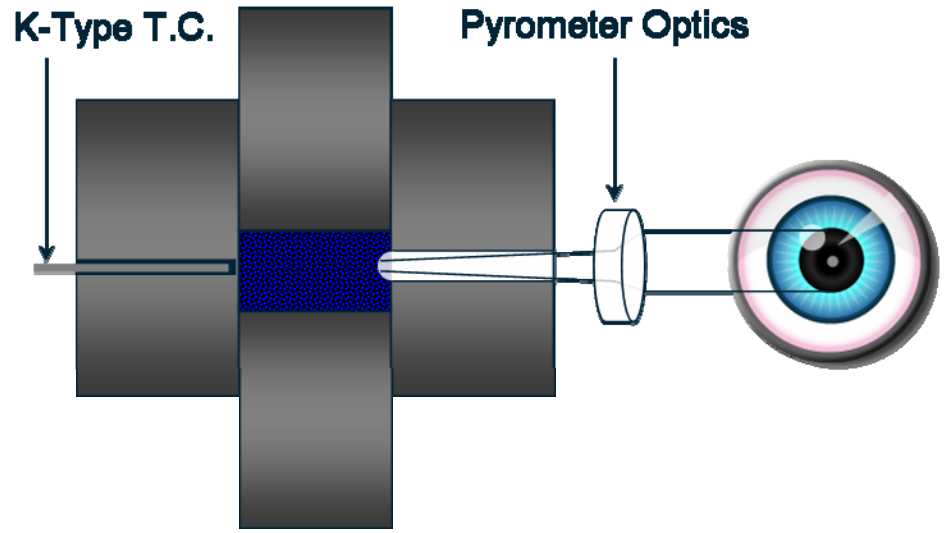
K-Type T.C.
Pyrometer Optics

Fig. 5

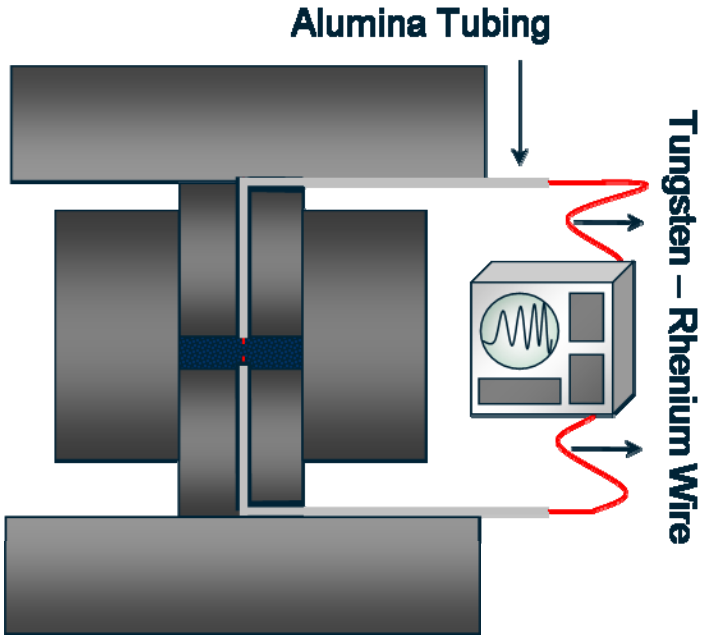
Alumina Tubing
Tungsten – Rhenium Wire

Fig. 6

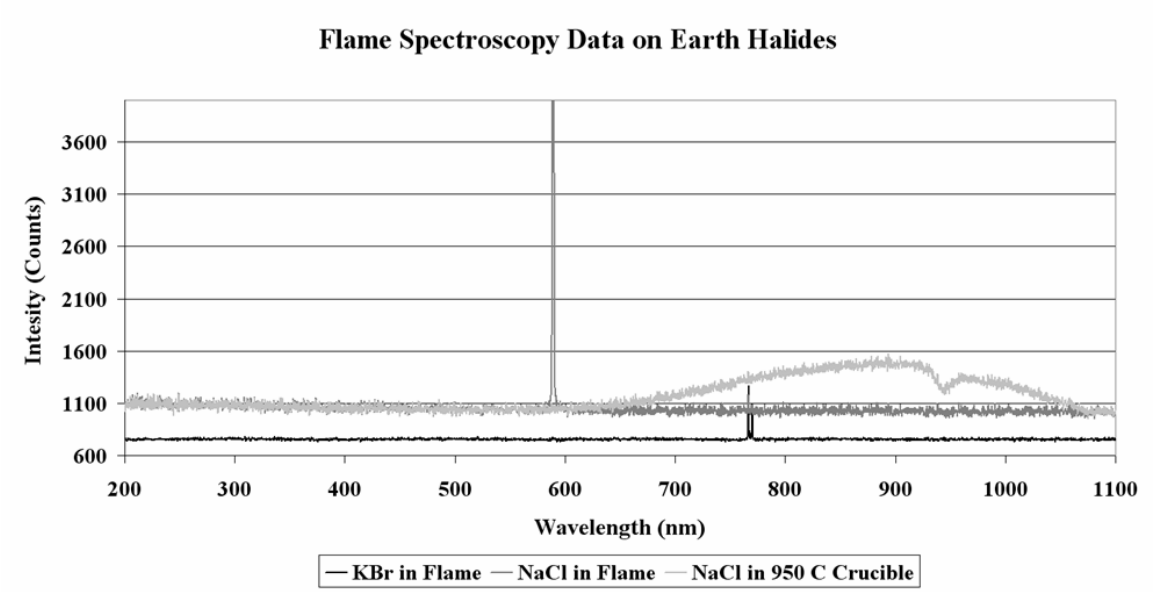
Flame Spectroscopy Data on Earth Halides
Intesity (Counts)
3600
3100
2600
2100
1600
1100
600
200
300
400
500
600
700
800
900
1000
1100
Wavelength (nm)
KBr in Flame
NaCl in Flame
NaCl in 950 C Crucible

Fig. 7

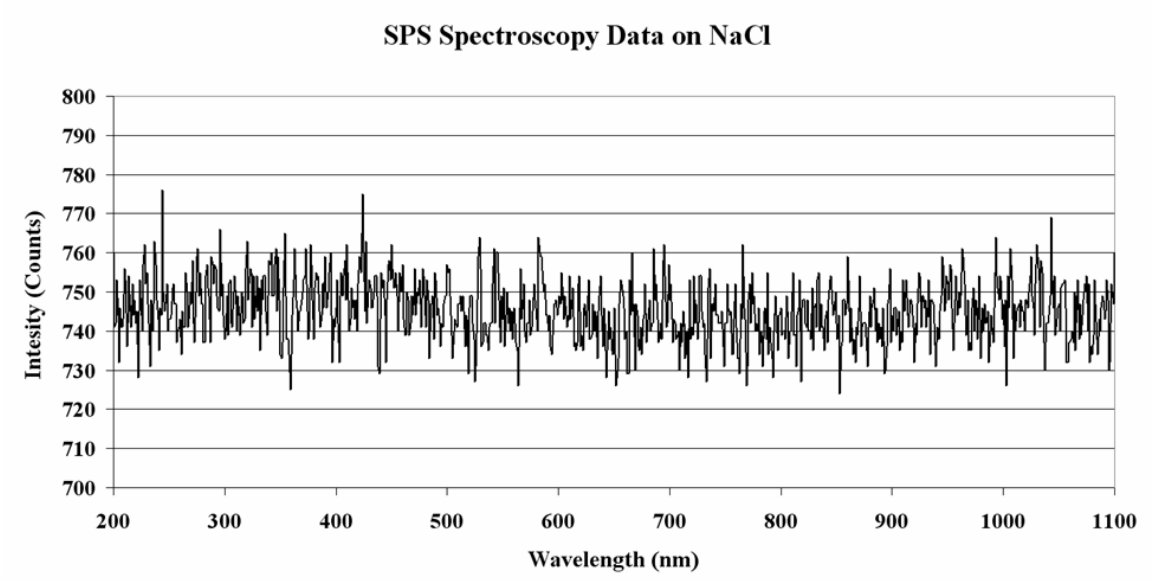
SPS Spectroscopy Data on NaCl
Intesity (Counts)
800
790
780
770
760
750
740
730
720
710
700
200
300
400
500
600
700
800
900
1000
1100
Wavelength (nm)

Fig. 8

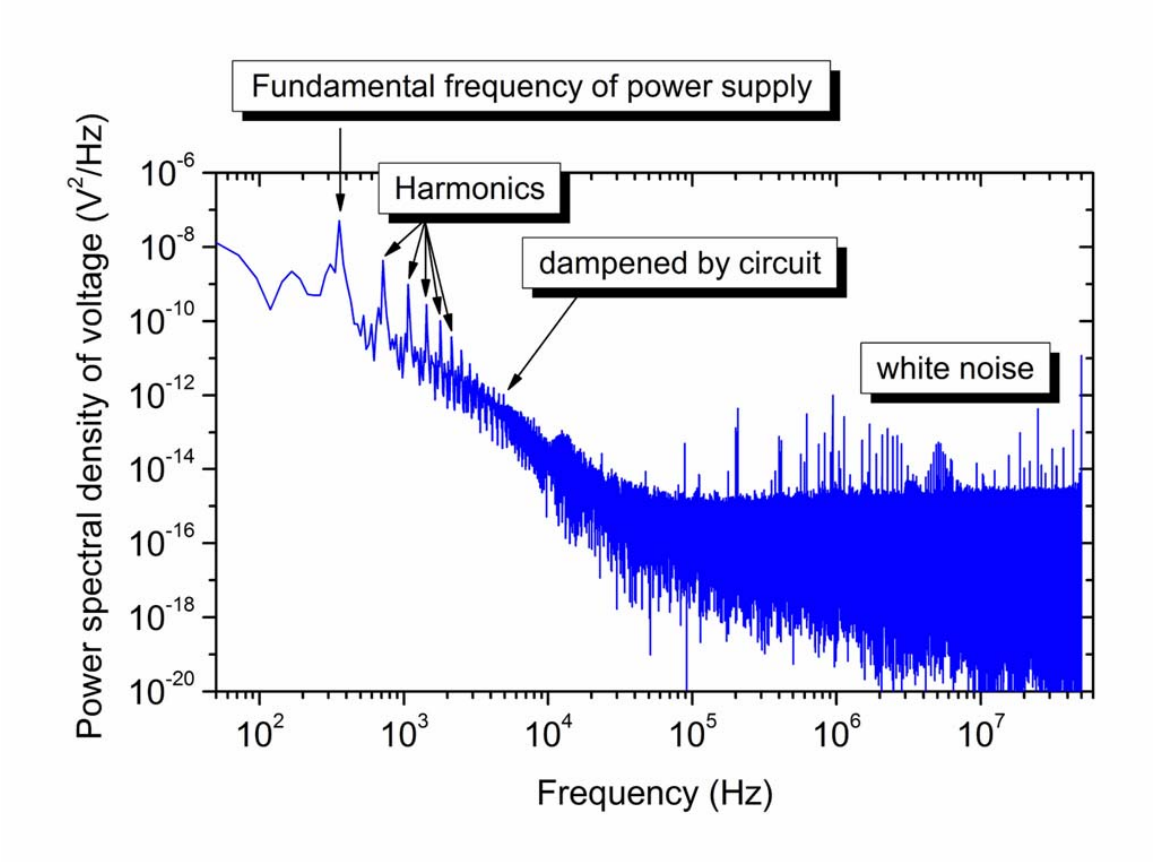
Fundamental frequency of power supply
Harmonics
dampened by circuit
white noise
Power spectral density of voltage (V²/Hz)
10⁻⁶
10⁻⁸
10⁻¹⁰
10⁻¹²
10⁻¹⁴
10⁻¹⁶
10⁻¹⁸
10⁻²⁰
10²
10³
10⁴
10⁵
10⁶
10⁷
Frequency (Hz)

Fig. 9

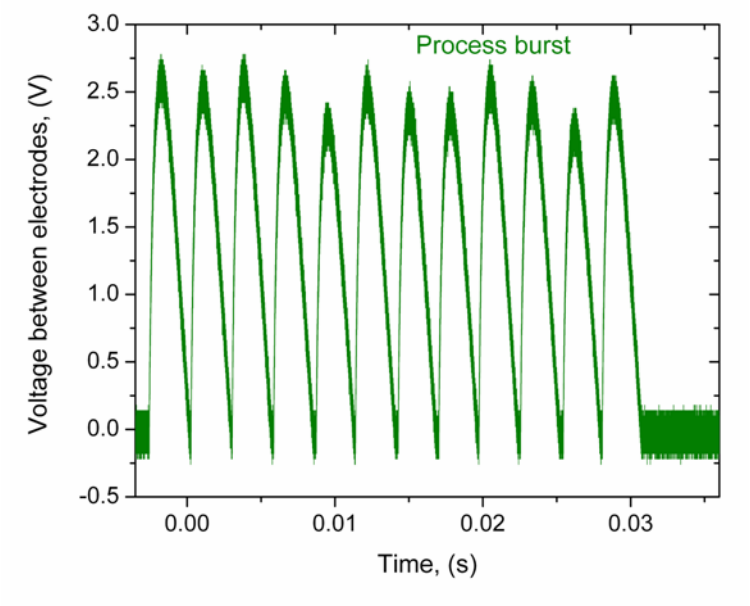
Process burst
Voltage between electrodes, (V)
Time, (s)
3.0
2.5
2.0
1.5
1.0
0.5
0.0
-0.5
0.00
0.01
0.02
0.03

Fig. 10

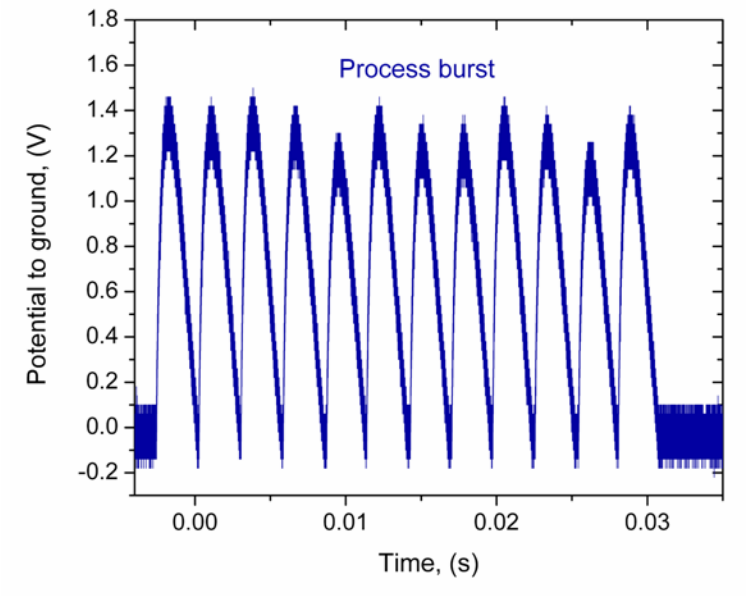
Process burst
Potential to ground, (V)
Time, (s)
1.8
1.6
1.4
1.2
1.0
0.8
0.6
0.4
0.2
0.0
-0.2
0.00
0.01
0.02
0.03

Fig. 11

TABLE

Table I - Sintering Conditions and Results of AES Experiments						
Powder	Temperature (°C)	Hold Time (min)	Pressure (MPa)	Forced Current	Atmosphere	Anomalous Radiation
None	650	1	14.2	N/A	Vacuum	No
Al	500	3	8.8	No	Vacuum	No
Al_2O_3	650	3	18	No	Vacuum	No
NaCl	650	3	5.7	No	Vacuum	No
Mg	450	3	6.1	No	Vacuum	No
Zn	225	2	16.2	Yes	Vacuum	No
Zn	275	2	16.2	Yes	Vacuum	No
Zn	225	2	13.3	Yes	Ar	No